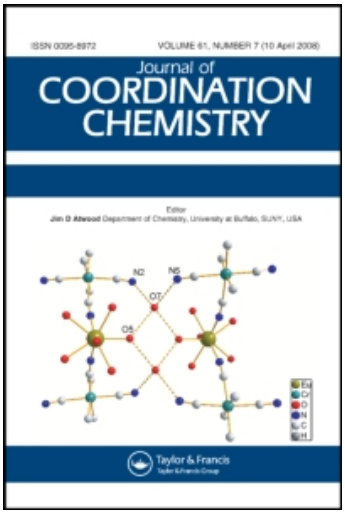

Journal of Coordination Chemistry
Publication details, including instructions for authors and subscription information:
http://www.informaworld.com/smpp/title~content=t713455674

Reactions of trivacant lone-pair-containing tungstobismutate and electrochemical behaviors of its sandwich-type products

Chun-Yan Sun[a]; Shu-Xia Liu[a]; Chun-Ling Wang[a]; Lin-Hua Xie[a]; Chun-Dan Zhang[a]; Bo Gao[a]; En-Bo Wang[a]
[a] Key Laboratory of Polyoxometalates Science of Ministry of Education, College of Chemistry, Northeast Normal University, Changchun, P.R. China

To cite this Article Sun, Chun-Yan , Liu, Shu-Xia , Wang, Chun-Ling , Xie, Lin-Hua , Zhang, Chun-Dan , Gao, Bo and Wang, En-Bo(2007) 'Reactions of trivacant lone-pair-containing tungstobismutate and electrochemical behaviors of its sandwich-type products', Journal of Coordination Chemistry, 60: 5, 567 — 579
To link to this Article: DOI: 10.1080/00958970600894972
URL: http://dx.doi.org/10.1080/00958970600894972

Journal of Coordination Chemistry
Vol. 60, No. 5, 10 March 2007, 567–579

Taylor & Francis
Taylor & Francis Group

Reactions of trivacant lone-pair-containing tungstobismutate and electrochemical behaviors of its sandwich-type products

CHUN-YAN SUN, SHU-XIA LIU*, CHUN-LING WANG, LIN-HUA XIE, CHUN-DAN ZHANG, BO GAO and EN-BO WANG

Key Laboratory of Polyoxometalates Science of Ministry of Education, College of Chemistry, Northeast Normal University, Changchun, 130024, P.R. China

(*Received in final form 6 July 2006*)

We report the crystal structure of dimeric precursor $Na_{12}[(Na(H_2O)_2)_6(\alpha\text{-}BiW_9O_{33})_2]$ (**1**), and the interaction of this precursor with transition metal ions. Interaction of **1** with Cu^{2+} in neutral medium leads to the formation of a Hervé-type sandwich polyoxoanion $[(Cu(H_2O))_3(\alpha\text{-}BiW_9O_{33})_2]^{12-}$ (**2**) in high yield. Interaction of **1** with M^{2+} (M = Zn, Ni, Co, Mn) in acidic aqueous medium leads to formation of Krebs-type sandwich polyoxoanions $[(M(H_2O)_3)_2(WO)_2(\beta\text{-}BiW_9O_{33})_2]^{10-}$ (**3**–**6**). Coordination geometry of the M^{2+} ions, counter-ions and precursors can affect the structure of products. In our experiments, only the interaction of **1** with Cu^{2+} forms a trisubstituted sandwich-type product. The method using $[\alpha\text{-}Bi^{III}W_9O_{33}]^{9-}$ as starting material is a convenient and effective route for the synthesis of sandwich-type tungstobismutates in high purity and yield. The electrochemical properties of these sandwich-type tungstobismutates in aqueous solution are described.

Keywords: Polyoxometalates; Tungstobismutate; Sandwich-type; Electrochemistry

1. Introduction

Polyoxometalates (POMs) have generated substantial interest in recent years because of structural variety and exciting properties [1–5]. To synthesize novel polyoxoanions with desired catalytic and magnetic properties, a widely used approach is to react trivacant heteropolyanion precursors with transition metal ions. The reactions of transition metal cations with trivacant POM species are very complex. First, the three substituted metal octahedra can be corner-sharing (A-type) or edge-sharing (B-type) [5]. Second, the Baker–Figgis isomerism affects the structure of products (in traditional Keggin structures, with 60° cap rotation isomers denoted as β, γ, δ, and ε for one, two, three, or four cap rotations, respectively [6]). Third, trivacant POMs can react with d-electron metals to form either the trisubstituted parent ('monomeric') structure or sandwich-type structures resulting from the fusion of two trivacant POMs units with transition metal ions. In addition, the number and connectivity of transition metals in sandwich-type structures vary.

*Corresponding author. Tel.: +86-431-5099765. Fax: +86-431-5684009. Email: liusx@nenu.edu.cn; liusx6789@yahoo.com.cn

Journal of Coordination Chemistry
ISSN 0095-8972 print/ISSN 1029-0389 online © 2007 Taylor & Francis
DOI: 10.1080/00958970600894972

Of particular interest are polyoxoanions containing a hetero group with a lone pair of electrons (e.g. As^{III}, Sb^{III}, and Bi^{III}). Different from the tetrahedrally coordinated heteroatoms P^{V}, As^{V}, Si^{IV} and Ge^{IV}, the heteroatoms As^{III}, Sb^{III} and Bi^{III} are surrounded pyramidally by three oxygen atoms [7]. They display interesting structures due to the stereochemical effect of the lone pair orbital electrons located on top of the trigonal pyramid [8]. This feature does not allow the closed Keggin unit to form. Some polyoxotungstates of this type have been structurally characterized, and most of them consist of dimeric adducts of incomplete Keggin units joined together by extra W or transition metal ions. In this class, several structurally characterized tungstobismutate have been reported, $[Bi_2W_{22}O_{74}(OH)_2]^{12-}$, its 3d transition-metal-disubstituted complexes $[Bi_2W_{20}M_2O_{70}(H_2O)_6]^{(14-2n)-}$ ($M = Co^{II}$, Mn^{II}, Zn^{II}, Ni^{II}, Cu^{II} and Fe^{III}), and the $Na_8(NH_4)_{2.5}[Sn_{1.5}\{WO_2(OH)\}_{0.5}(WO_2)_2(BiW_9O_{33})_2]\cdot 36.5H_2O$ complexes composed of trivacant β-B-BiW_9O_{33} units [8–12]; the polyanion $[H_3BiW_{18}O_{60}]^{6-}$ [13], and the compounds $Na_9[\{Na(H_2O)_2\}_3\{Cu(H_2O)\}_3(BiW_9O_{33})_2]\cdot 42H_2O$ [14] containing α-B-BiW_9O_{33} units. In addition, in 2001, Rusu reported FT-IR, UV–vis and EPR investigations of multicopper polyoxotungstates with Bi^{III} as heteroatom [15]. The same group synthesized $[M^{n+}{}_3(H_2O)_x(BiW_9O_{33})_2]^{(18-3n)-}$ ($M^{n+} = (VO)^{II}$, $x = 0$ and $M^{n+} = Cr^{III}$, Mn^{II}, Fe^{III}, Co^{II}, Ni^{II}, Cu^{II}, $x = 3$) [16], however, the proposed formulas and structures remain to be confirmed by X-ray diffraction. Complex reaction mechanisms are responsible for these distinct trivacant lone-pair-containing subclass POMs, making a straightforward reaction route for their syntheses difficult, even in apparently simple cases.

In this context, our research focuses on the investigation of reactions of trivacant tungstobismutates with transition metals. We report the dimeric precursor $[(Na(H_2O)_2)_6(\alpha\text{-}BiW_9O_{33})_2]^{12-}$ (**1**) an analogue of an antimony complex that was not structurally characterized, and investigated the reactions of this precursor with transition metal ions. Although there are many variables in the synthesis, only two kinds of sandwich-type classes (**2** belongs to Krebs-type and **3**–**6** belong to Hervé-type) can be obtained in our experiments. We have also studied for the first time in a systematic way the electrochemical behavior of compounds **1**–**6** in aqueous solution.

2. Experimental section

2.1. *General methods*

All chemicals were of reagent grade and used as purchased commercially. Elemental analyses (Cu, Zn, Ni, Mn, Co, Na, W) were determined on a Leaman inductively coupled plasma (ICP) spectrometer. IR spectra were obtained on a Nicolet 205 FT/IR spectrometer with KBr pellets in the 400–4000 cm^{-1} region. TG analyses were performed on a Perkin-Elmer TGA7 instrument in flowing N_2 with a heating rate of $10^{\circ}C\,min^{-1}$. UV–vis spectra were recorded on a 756 CRT UV–vis spectrophotometer. The UV spectra were recorded using aqueous solutions (0.015–0.052 mM) of the POMs; spectra for the visible region were collected using 5.5×10^{-3}–0.1 mol L^{-1} aqueous solutions. The compositions of the various media follow: pH 4 and 5 : 0.4 mol L^{-1} $CH_3COONa + CH_3COOH$; for pH 7 : 0.4 mol L^{-1} $NaH_2PO_4 + NaOH$.

Cyclic voltammetry measurements were carried out on a CHI 660 electrochemical workstation using a conventional three-electrode single compartment cell at room temperature. The working electrode was a glassy carbon disc electrode or a homemade platinum foil electrode. The surface of the glassy carbon electrode was polished with 0.3 μm alumina and washed with distilled water before each experiment. Platinum gauze was used as a counter electrode and Ag/AgCl was used as reference electrode. The solutions were degassed with pure nitrogen for 15 min before use and blanketed with nitrogen gas during the voltammetric scans. Controlled potential electrolysis experiments were performed using an AUTOLAB PGSTAT 30 potentiostat. The reference electrode was the same as above. A carbon cloth or a platinum mesh was used as the working electrode. The counter electrode was platinum mesh of large surface area. Spectroelectrochemical experiments were performed on a UNICAM UVI spectrophotometer connected to an AUTOLAB PGSTAT 30 potentiostat, using a quartz cuvette (4 cm optical path). The three-electrode system was inserted in the cell and kept under continuous nitrogen bubbling and stirring during electrolysis. The working electrode was a platinum foil. Experiments were performed at room temperature.

2.2. *Synthesis of compounds*

The total number of water molecules in the complexes has been determined by thermogravimetry.

$Na_{12}[(Na(H_2O)_2)_6(\alpha\text{-}BiW_9O_{33})_2] \cdot 27H_2O$ (1). $Na_2WO_4 \cdot 2H_2O$ (40 g, 121 mmol) was dissolved in 150 mL of hot water (80°C, pH 8.5). Hydrochloric acid (6 mol L^{-1}) was added dropwise with stirring to the tungstate solution to adjust the pH to 7. Then $Bi(NO_3)_3 \cdot 5H_2O$ (6.5 g, 13.4 mmol) dissolved in HCl (6 mol L^{-1}, 10 mL) was added dropwise to the tungstate solution with vigorous stirring. Precipitate formed during the addition but dissolved immediately, and the solution became yellow. The mixture was refluxed for 1 h and allowed to cool slowly. Colourless crystals were obtained upon cooling at room temperature. Yield: 29 g (74.5%); Anal. Calcd for $Na_{12}[Na_6Bi_2W_{18}O_{66}(H_2O)_{12}] \cdot 27H_2O$ (%): W, 56.09; Bi, 7.08; Na, 7.01. Found: W, 56.04; Bi, 7.10; Na, 7.00. IR (KBr pellet, cm^{-1}): 947, 879, 725, 669 cm^{-1}.

$Na_{18}[(Cu(H_2O))_3(\alpha\text{-}BiW_9O_{33})_2] \cdot 56H_2O$ (2). 2.9 g (1 mmol) compound **1** was dissolved in 30 mL of H_2O (60°C), and then 0.45 g (2 mmol) $CuCl_2 \cdot 5H_2O$ dissolved in minimal water was added. The pH of the solution was adjusted to 7.0 by addition of 3 M HCl. The mixture was heated at 60°C for another 1 h. The resulting bright-green solution was filtered and allowed to cool at ambient temperature. Green block crystals of desired product were obtained within 3 days. Anal. Calcd for $Na_{18}[Cu_3Bi_2W_{18}O_{66}(H_2O)_3] \cdot 56H_2O$ (%): W, 51.30; Cu, 2.95; Bi, 6.48; Na, 6.41. Found: W, 51.40; Cu, 3.07; Bi, 6.50; Na, 6.47. IR, (KBr pellet, cm^{-1}): 946, 860, 750, 690 cm^{-1}.

Compounds 3–6. 5.7 g (2 mmol) compound **1** was dissolved in 30 mL of 1 mol L^{-1} hot sodium acetate buffer solution (pH 4.8, 60°C), and then the transition metal salts (2 mmol) dissolved in minimal water was added dropwise. The mixture was heated

to 80–85°C for 1 h. The resulting solution was filtered through a medium frit and allowed to cool at ambient temperature. Crystals of the desired products were obtained within one day to one week.

$Na_{10}[Bi_2W_{20}Zn_2O_{70}(H_2O)_6] \cdot 40H_2O$ (3). The colourless crystal was prepared using $Zn(NO_3)_2 \cdot 6H_2O$ (2 mmol). (Yield: ca 75% based on Zn). Anal. Calcd for $Na_{10}[Bi_2W_{20}Zn_2O_{70}(H_2O)_6] \cdot 40H_2O$ (%): W, 57.41; Zn, 2.04; Bi, 6.53; Na, 3.59. Found: W, 56.52; Zn, 2.02; Bi, 6.49; Na, 3.54. IR: (KBr pellet, cm^{-1}): 946, 830, 700, 605 cm^{-1}.

$Na_{10}[Bi_2W_{20}Ni_2O_{70}(H_2O)_6] \cdot 31H_2O$ (4). The green crystal was prepared using $Ni(CH_3COO)_2 \cdot 4H_2O$ (2 mmol). (Yield: ca 77% based on Ni). Anal. Calcd for $Na_{10}[Bi_2W_{20}Ni_2O_{70}(H_2O)_6] \cdot 31H_2O$ (%): W, 59.03; Ni, 1.88; Bi, 6.71; Na, 3.69. Found: W, 59.37; Ni, 1.86; Bi, 6.65; Na, 3.65. IR: (KBr pellet, cm^{-1}): 944, 816, 630 cm^{-1}.

$Na_{10}[Bi_2W_{20}Mn_2O_{70}(H_2O)_6] \cdot 26H_2O$ (5). The yellow crystal was prepared using $MnSO_4 \cdot 2H_2O$ (2 mmol). (Yield: ca 69% based on Mn). Anal. Calcd for $Na_{10}[Bi_2W_{20}Mn_2O_{70}(H_2O)_6] \cdot 26H_2O$ (%): W, 59.97; Mn, 1.79; Bi, 6.82; Na, 3.75. Found: W, 59.80; Mn, 1.70; Bi, 6.79; Na, 3.96. IR (KBr pellet, cm^{-1}): 940, 820, 650, 599 cm^{-1}.

$Na_{10}[Bi_2W_{20}Co_2O_{70}(H_2O)_6] \cdot 30H_2O$ (6). The pink crystal was prepared using $Co(CH_3COO)_2 \cdot 2H_2O$ (2 mmol). (Yield: ca 90% based on Co). Anal. Calcd for $Na_{10}[Bi_2W_{20}Co_2O_{70}(H_2O)_6] \cdot 30H_2O$ (%): W, 59.20; Co, 1.90; Bi, 6.73; Na, 3.70. Found: W, 59.30; Co, 1.90; Bi, 6.87; Na, 3.74. IR (KBr pellet, cm^{-1}): 940, 820, 637 cm^{-1}.

As the quality of the crystals of **5** and **6** was not good enough for single crystal X-ray analysis the obtained structural data were not given here, though they confirmed the reported structure. Also the analytical, spectroscopic data are identical.

2.3. *X-ray crystallographic study*

The reflection intensity data for all compounds were collected on a Rigaku R-AXIS RAPID IP diffractometer with graphite monochromated Mo-Kα radiation at 293 K, and an empirical absorption correction by SADABS was applied to the intensity data. All the structures were solved by direct methods and refined using the full-matrix least-squares method on F^2 with SHELXTL crystallographic software package. A summary of the crystallographic data and structure refinement for compounds **1**–**4** is given in table 1.

Table 1. Crystal data and structure refinement for compounds **1**–**4**.

	1	**2**	**3**	**4**
Empirical formula	$H_{39}BiNa_9O_{52.5}W_9$	$H_{118}Bi_2Na_{18}Cu_3O_{125}W_{18}$	$H_{46}BiNa_5ZnO_{58}W_{10}$	$H_{37}BiNa_5NiO_{53.5}W_{10}$
Formula weight	2949.54	6312.70	3245.01	3149.72
Temperature (K)	293(2)	293(2)	293(2)	293(2)
Space group	$P\bar{1}$	$P\bar{1}$	$P2(1)/n$	$P2(1)/n$
a (Å)	11.552(3)	13.674(3)	12.9216(6)	12.9018(5)
b (Å)	13.840(4)	13.689(3)	25.2298(11)	25.2129(3)
c (Å)	17.103(3)	31.931(6)	16.2070(7)	16.0755(6)
α (°)	66.512(3)	94.21(3)		
β (°)	82.556(3)	94.40(3)	94.4560(10)	94.00(10)
γ (°)	69.759(3)	117.80(3)		
V (Å^3)	2352.8(10)	5231.2(18)	5267.7(4)	5216.5(3)
Z	2	2	4	4
D_{calcd} (mg m^{-3})	4.108	4.008	4.092	4.011
μ (mm^{-1})	25.837	23.836	25.680	25.821
$F(000)$	2536	5670	5842	5624
Reflection collected	12554	49126	28207	27334
Independent reflections	8181	23346	9522	9173
R_1, wR_2 [$I>2\sigma(I)$]	0.0353, 0.0874	0.0569, 0.1128	0.0550, 0.1358	0.0697, 0.1638
R_1, wR_2 (all data)	0.0483, 0.0937	0.0867, 0.1255	0.0626, 0.1390	0.0886, 0.1685

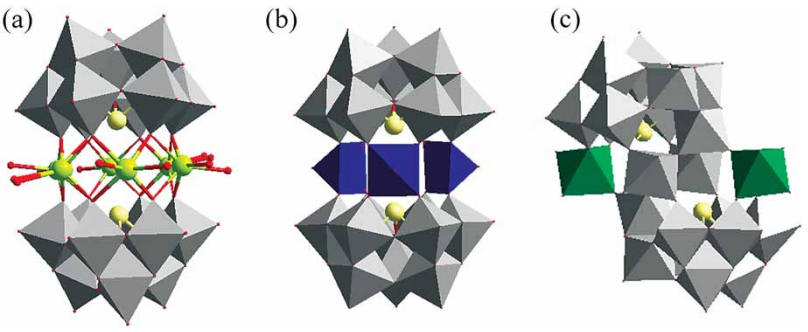

Figure 1. (a) Combined polyhedron/ball-and-stick representation of $[(Na(H_2O)_2)_6(BiW_9O_{33})_2]^{12-}$ (**1**); (b) polyhedron plot of the molecular structure of $[(Cu(H_2O))_3(BiW_9O_{33})_2]^{12-}$ (**2**); (c) polyhedron plot of the molecular structure of $[(M(H_2O)_3)_2(WO_2)_2(BiW_9O_{33})_2]^{10-}$ ($M = Ni^{2+}$, Zn^{2+}, Co^{2+}, Mn^{2+}) (**3**–**6**). Bi^{III} (cream-coloured), Na (yellow), O (red), WO_6 (gray octahedra), CuO_5 (blue polyhedron), MO_6 (green octahedra).

3. Results and discussion

3.1. *Synthesis and structure*

The X-ray structure analysis of $Na_{12}[(Na(H_2O)_2)_6(\alpha\text{-}BiW_9O_{33})_2]\cdot 27H_2O$ (**1**) reveals that in the crystal network of **1**, two α-B-$[BiW_9O_{33}]^{9-}$ anions related to each other by a center of inversion face each other with their open sites. A belt of six Na^+ ions connects both anions (figure 1a). Compound **1** has a similar structure to $Na_9[SbW_9O_{33}]$ [17], showing a rather close analogy between BiW and SbW systems. Compound **2** belongs to the class of Hervé-type sandwich POMs. The first member of this class $[Cu_3(H_2O)_2(\alpha\text{-}AsW_9O_{33})_2]^{12-}$] was reported by Hervé *et al.* [18]. Compound **2** consists of two α-B-$[BiW_9O_{33}]^{9-}$ moieties linked by three equivalent Cu^{2+} ions, resulting in a sandwich-type structure with idealized D_{3h} symmetry (figure 1b). Three equivalent Cu^{2+} ions, each coordinating a terminal water molecule result in square-pyramidal coordination. The three vacancies in the central belt were occupied by sodium. Compounds **3**–**6** belong to the Krebs-type sandwich POMs which is based on two lone pair-containing, β-Keggin units. The first members of this class $[M_2(H_2O)_6(WO_2)_2(\beta\text{-}SbW_9O_{33})_2]^{(14-2n)-}$ ($M = Fe^{3+}$, Co^{2+}, Mn^{2+}, Ni^{2+}) were reported by Krebs *et al.* [19]. Compound **3**–**6** are composed of two β-B-$[BiW_9O_{33}]^{9-}$ fragments joined together by two corner-sharing WO_6 octahedra and two octahedral $M^{II}O_3(H_2O)_3$ ($M = Ni^{II}$, Zn^{II}, Mn^{II}, Co^{II}) groups. A view of the anion is shown in figure 1c. In **2**–**6**, all the anions are linked in chain by sodium cations (figure 2).

Compound **2** was synthesized in neutral aqueous medium from precursor **1**, isostructural with the $Na_{12}[Sb_2W_{18}Cu_3O_{66}(H_2O)_3]\cdot 46H_2O$ (**2′**) and $Na_{12}[As_2W_{18}Cu_3O_{66}(H_2O)_3]\cdot 32H_2O$ (**2″**) [19]. The separations of the three copper ions and the two heteroatoms in polyanions with different compounds are summarized in table 2. When comparing compounds **2**, **2′** and **2″**, it can be noted that all have the same charge, but the size of heteroatom is different: **2** > **2′** > **2″**. The average equatorial Cu–O_{ax} distances in polyanions **2**–**2″** are similar (**2**, 1.940(6) Å; **2′**, 1.937(6) Å; **2″**, 1.921(6) Å), so that the differences in the Cu···Cu separations of **2**–**2″** must be due to an 'equatorial expansion motion' of the polyanion in the belt region. We believe that this is caused by lone pair/lone pair interaction of the two heteroatoms, which is more

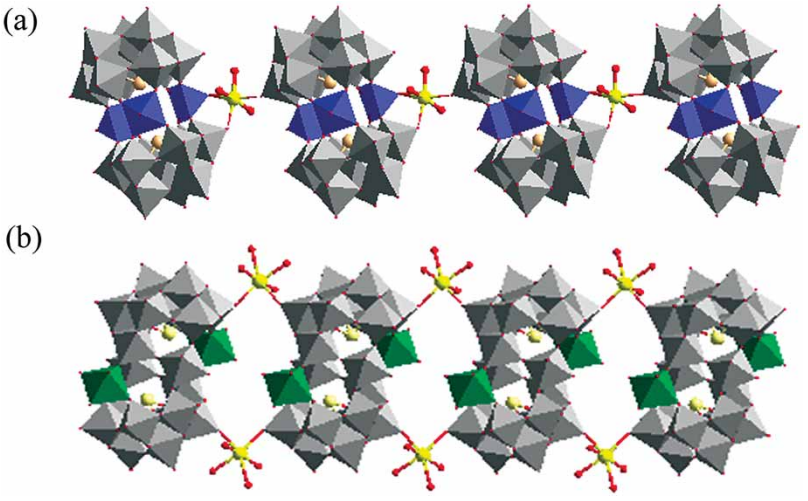

Figure 2. Combined polyhedral/ball-and-stick representation of the 1-D chains in (a) **2**, (b) **3**–**6**. Bi^{III} (cream-coloured), Na (yellow), O (red), WO_6 (gray octahedra), CuO_5 (blue polyhedron), MO_6 ($M = Ni^{2+}$, Zn^{2+}, Co^{2+}, Mn^{2+}) (green octahedra).

Table 2. Cu···Cu and heteroatom (X···X) separations in polyanions in different compounds.

Polyanion	Cu···Cu (Å)	X···X (Å) (X = Bi, Sb, As)
$[Cu_3(H_2O)_3(\alpha\text{-}BiW_9O_{33})_2]^{12-}$ (**2**)	4.89	4.55
$[Cu_3(H_2O)_3(\alpha\text{-}SbW_9O_{33})_2]^{12-}$ (**2′**)	4.84	4.85
$[Cu_3(H_2O)_3(\alpha\text{-}AsW_9O_{33})_2]^{12-}$ (**2″**)	4.69	5.34

pronounced in **2** than in **2′** and **2″**. Use of KCl, resulted in no crystal, indicating that sodium ions stabilize Cu^{2+} substituted, sandwich-type polyoxotungstate complexes of Bi^{III}, consistent with the observed arsenic and antimony analogues [19]. Using this method, compounds **3**–**6** with structures previously reported [9–11] can also be obtained. Polyanions **3**–**6** were synthesized in aqueous acidic medium (pH 5) from an interaction of M^{2+} ions with the precursor **1**. Therefore, the mechanism of formation of **3**–**6** involves insertion, isomerization ($\alpha \rightarrow \beta$), and dimerization. It was shown by Krebs *et al*. that α-$[SbW_9O_{33}]^{9-}$ and β-$[SbW_9O_{33}]^{9-}$ are in equilibrium in aqueous solution [19]. The former dominates in neutral medium whereas the latter is present in acidic solution. We propose that the behavior of α-$[BiW_9O_{33}]^{9-}$ and β-$[BiW_9O_{33}]^{9-}$ is very similar to their antimony analogues.

We were unable to synthesize other transition metal derivatives of **2** under the same conditions. These observations suggest that the coordination requirements of the transition metal ions play an important role in the formation of the two structural types. The coordination geometry of the Zn^{2+}, Ni^{2+}, Co^{2+}, Mn^{2+} ions in **3**–**6** are octahedral, whereas the structure of **2** requires square pyramidal coordination geometry for Cu^{2+}. Another reason for the formation of the different POMs as the d-metal is varied may be that there is often a significant difference in the size of a d-electron containing transition metal ions and size of the 'hole' in

Table 3. Average bond lengths of transition metal center in compounds **2**–**5**.

Compounds	**2**	**3**	**4**	**5**
Metal center	Cu	Zn	Ni	Mn
$M–O_{ax}$[a]	1.940(2) Å	2.056(4) Å	2.048(1) Å	2.112(4) Å
$M–O_{eq}$[a]	2.224(1) Å	2.122(3) Å	2.086(1) Å	2.195(4) Å
ΔM–O[b]	0.28 Å	0.066 Å	0.038 Å	0.083 Å

[a]Average (axial and equatorial) Cu–O, Zn–O, Ni–O, and Mn–O bond lengths, respectively, for the MO_6 octahedra in the central unit.
[b]Differences in average axial and equatorial M–O bond lengths.

POM unit (for example, the radius of octahedrally coordinated W^{VI} is 0.74 Å, while that of high-spin octahedral Co^{II} is 0.885 Å). The larger d-electron-containing metal centers might be better accommodated by sandwich-type structures on the exterior. The other reason may relate to the Jahn–Teller effect. Table 3 provides bond lengths for the d-metal centers in **2**–**5** that define the degree of Jahn–Teller distortion in each (differences in the axial and equatorial M-O bonds). Cu^{II} center in compound **2** shows significant Jahn–Teller distortion, which impacts the stoichiometry of its incorporation and connectivity.

The reactions starting with sodium orthotungstate have also been carried out for synthesis, and again only the interaction of sodium tungstate with Cu^{2+} can form the trisubstituted sandwich-type product. However, the yield and purity of the crystals obtained by the alternative preparation method were significantly lower. So the method described here using compound **1**, is a reliable and effective way for the synthesis of sandwich-type tungstobismutates.

3.2. *IR spectra*

Some information about the coordination and local symmetry of M^{2+} in the compounds can be obtained by comparing the FT-IR spectra of the sandwich-type complexes and those of **1** (figure 3). Compound **2** has three main absorptions at 946(vs), 860(vs), and 690(vs) cm^{-1}, attributed to the characteristic absorption of $\nu(W–O_d)$, $\nu(W–O_b)$ and $\nu(W–O_c)$, repectively. Although the bands for $W–O_b$ and $W–O_c$ tend to split, they can be distinguished clearly. However, for compounds **3**–**6**, as the symmetry of complexes decreased to C_{2v} from D_{3h}, the coordination of $O_{b/c}$ became complex. As a result, the bands of $W–O_b$ and $W–O_c$ merge providing a method for distinguishing these two types of polyanions.

3.3. *Electrochemistry*

The stability of the polyanions **1**–**6** between pH 4 and 7 was checked using UV–Vis spectroscopy. The spectra of all compounds were completely reproducible with respect to absorbance and wavelengths over a period of at least 24 h. The electrochemical studies of **1**–**6** were performed by cyclic voltammetry. In this short account, only results in a single pH 5 medium have been used.

The evolution of the cyclic voltammograms of **1** and **2** are presented in figure 4. The pattern of **1** shows a system of two closely spaced one-electron waves, featuring the first

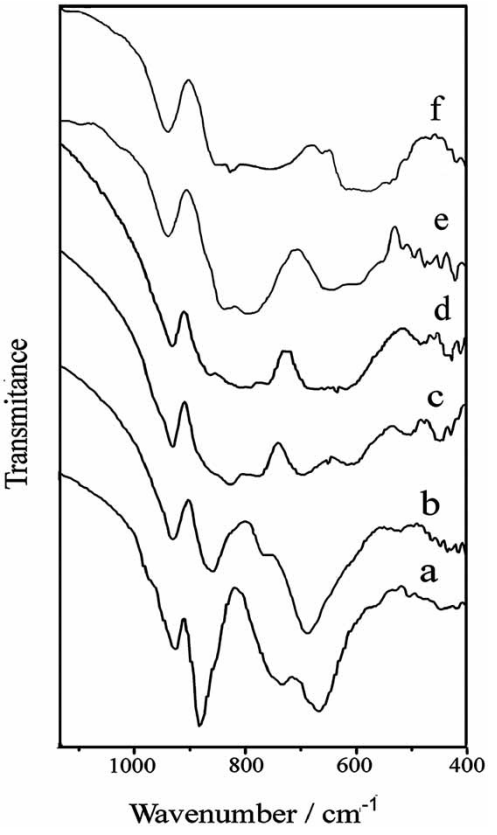

Figure 3. IR spectra of sandwich complexes: (a) **1**, (b) **2**, (c) **3**, (d) **4**, (e) **5** and (f) **6**.

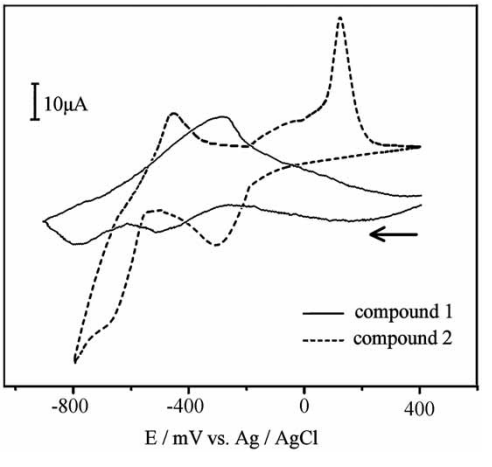

Figure 4. Cyclic voltammetry of aqueous solution of compounds **1** and **2** at pH 5 (0.4 mol L^{-1} CH_3COONa and CH_3COOH) (scan rate = 20 mV s^{-1}).

Table 4. Cyclic voltammetric data or polyanions in pH 5 aqua solution.[a]

		M[b]	W[c] (1st)	W[c] (2nd)	W[c] (3rd)
Polyoxoanion	E_c	E_a	E_c (ΔE_p)	E_c (ΔE_p)	E_c (ΔE_p)
$Co^{II}_2(BiW_9)_2$	423, 529	439, 581	−398 (95)	−460 (125)	−508 (83)
$Mn^{II}_2(BiW_9)_2$		391, 509	−309 (100)	−463 (90)	−537 (109)
$Ni^{II}_2(BiW_9)_2$			−311 (92)	−420 (112)	−499 (88)
$Zn^{II}_2(BiW_9)_2$			−298 (80)	−381 (90)	−552 (100)
$Cu^{II}_3(BiW_9)_2$	−310	0, 186	−653 (133)		

[a]Cathodic (E_c) and anodic (E_a) peak potentials and cathodic-to-anodic peak separation (ΔE_p) in mV *vs.* Ag/AgCl; polyoxoanion concentration: 5.0×10^{-3} mol L^{-1}; 0.4 mol L^{-1} sodium acetate buffer solution; scan rate: 20 mV s^{-1}.
[b]Platinum foil electrode.
[c]Glassy carbon electrode.

two reduction processes of the W centers. Upon potential reversal, a single oxidation wave is obtained. In contrast with the voltammograms of **1**, those of **2** show a new wave with large current in the potential domain −310 mV. This new wave is attributed to reduction of the three Cu^{II} centers within the sandwich complex. Controlled potential coulometry confirmed the uptake of three electrons for this wave. Reversal of the potential scan just before the beginning of the third wave system indicates three oxidation waves. The two less negative oxidation waves are attributed to the oxidation of copper, thus reinforcing the idea that discrete but very close reduction potentials should exist for the Cu^{2+} centers. One of them is clearly an adsorptive oxidation process and its shape indicates that deposition of copper occurred during the negative scan. The W waves also mix up, and the system of two one-electron waves is replaced by a single two-electron wave.

Cyclic voltammetry between 1000 and −1000 mV for compounds **3**–**6** reveals no significant changes upon varying the scan rate from 20 to 200 mV s^{-1}. For potentials <−200 mV three waves, corresponding to tungsten reductions (table 4), were observed. Controlled potential electrolysis revealed that each of the first two W reduction peaks corresponded to one-electron transfer processes. The number of electrons of the third W reduction was estimated to be two, by comparison of the current of the corresponding voltammetric peak with those of the first and second reductions. Thus, the tungsten-oxo framework of the heteropolyanions studied could accept four electrons, within the present experimental potential range. Figure 5 presents the voltammogram of $Zn_2(BiW_9)_2$ (roughly similar to those of the Co^{II}, Mn^{II}, Ni^{II} derivatives).

Oxidation processes at Co^{II} and Mn^{II} can be observed. For the Co^{II} sandwich polyoxoanion, two oxidation peaks of identical intensity were detected at +439 and +581 mV (figure 6a). In corresponding reduction scan, the two cathodic peaks which are the counterparts can be observed. Electrolysis of the $Co_2(BiW_9)_2$ solution at the Pt electrode with coulometric determination, performed at +480 mV, indicated the transfer of 0.8 electrons, meaning that each oxidation peak corresponds to a one-electron process (total loss of two electrons). The shape of the cyclic voltammograms was not altered either by change of scan rate or by multiple successive scans. The *in situ* visible spectra of the oxidized solution revealed a new band around 660 nm for $Co_2(BiW_9)_2$, indicating a $Co^{III}O_6$ chromophore [20]. From the above considerations the

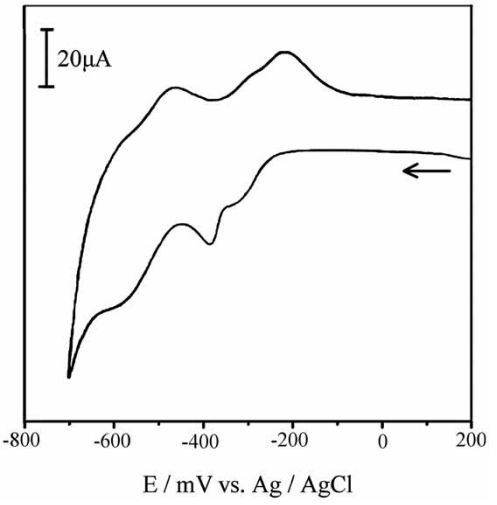

Figure 5. Cyclic voltammetry at a glassy carbon working electrode of an aqueous solution of $Zn^{II}_2(BiW_9)_2$ at pH 5 (0.4 mol L^{-1} CH_3COONa and CH_3COOH) (scan rate = 20 mV s^{-1}) in the negative potential region.

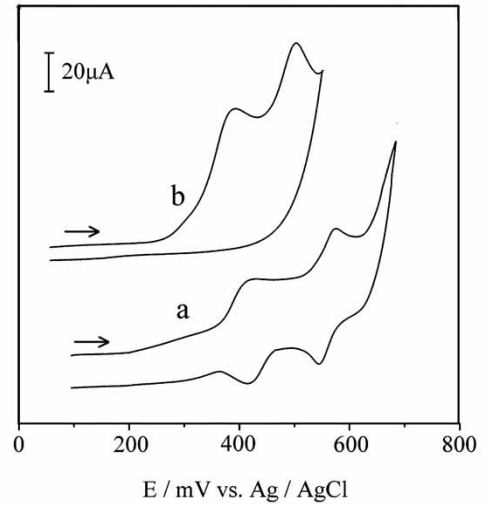

Figure 6. (a) Cyclic voltammetry at a Pt foil working electrode of solutions of: (a) $Co^{II}_2(BiW_9)_2$; (b) $Mn^{II}_2(BiW_9)_2$ (scan rate = 20 mV s^{-1}) at pH 5 (0.4 mol L^{-1} CH_3COONa and CH_3COOH) in the positive potential region.

cobalt oxidation processes can be described as:

$$[Co^{II}Co^{II}(BiW_9)_2]^{10-} \rightarrow [Co^{III}Co^{II}(BiW_9)_2]^{9-} + e^- \quad (1)$$

$$[Co^{III}Co^{II}(BiW_9)_2]^{9-} \rightarrow [Co^{III}Co^{III}(BiW_9)_2]^{8-} + e^- \quad (2)$$

$Mn_2(BiW_9)_2$ shows two irreversible oxidation processes at the Mn center (figure 6b), with the total electron transfer of two electrons (value obtained by electrolysis with

coulometric determination at +590 mV using the Pt electrode), and attributed to slow electron transfer, rather than to chemical irreversibility [21]. The bands at 483 and 540 nm (sh) of oxidized solution of $Mn_2(BiW_9)_2$ confirm the $Mn^{III}O_6$ chromophore [22, 23]. Tentatively, the separation of the oxidation potentials of Co^{II} or Mn^{II} centers might be attributed to electronic interactions involving the central heteroatoms. Apparently, this interaction generates inequivalence among the Co^{II} or Mn^{II} centers. In the potential domains explored, no electrochemical activity has been detected for Ni^{II} or Zn^{II}.

4. Conclusion

Interactions of dimeric precursor $Na_{12}[(Na(H_2O)_2)_6(\alpha\text{-}BiW_9O_{33})_2]$ (**1**) with transition metal ions were studied. Using this method the Hervé-type sandwich polyanion $[(\alpha\text{-}BiW_9O_{33})_2Cu^{II}_3(H_2O)_3]^{12-}$ and Krebs-type sandwich polyanions $[M_2(H_2O)_6(WO_2)_2(\beta\text{-}BiW_9O_{33})_2]^{10-}$ ($M = Zn^{2+}$, Ni^{2+}, Co^{2+}, Mn^{2+}) can be obtained in high yield and purity. Interestingly, the structural type ($\alpha\alpha$) was not formed with other transition metal ions (Zn^{II}, Ni^{II}, Mn^{II}, Co^{II}). The fact that for other transition metal ions the same structural type ($\beta\beta$) is obtained, no matter what the precursors are, indicates boundary conditions present during the reaction determine which product is formed. On the other hand, the acidity of the reaction medium and the preferred coordination geometry of the incorporated transition metal seem to be more important. Cyclic voltammetry and controlled potential coulometry reveal that in the potential domains explored, the stepwise oxidation of Mn^{II} and Co^{II} can be observed.

Supplementary material

Crystal structure investigations of **1**–**4** may be obtained from the Fachinformationszentrum Karlsruhe, D-76344 Eggenstein-Leopoldshafen, Germany (Email: Crysdata@fiz-karlstruhe.de) on quoting the deposited numbers CSD-416153, CSD-416151, CSD-416149 and CSD-416150, respectively.

Acknowledgements

This work was supported by the National Science Foundation of China (Grant No. 20571014) and the Scientific Research Foundation for Returned Overseas Chinese Scholars, the Ministry of Education.

References

[1] *Chem. Rev.*, **98**, 1, Thematic issue on polyoxometalates (1998).
[2] M.T. Pope, A. Müller (Eds). *Polyoxometalate Chemistry*: *From Topology via Self-assembly to Applications*, Kluwer, Dordrecht, the Netherlands (2001).

[3] M.T. Pope (Ed.). *Polyoxometalates*: *From Platonic Solids to Anti-retroviral Activity*, Kluwer, Dordrecht, the Netherlands (1994).
[4] M.T. Pope, A. Müller. *Angew. Chem., Int. Ed. Engl.*, **30**, 34 (1991).
[5] M.T. Pope (Ed.). *Heteropoly and Isopoly Oxometalates*, Springer-Verlag, Berlin (1983).
[6] L.C.W. Baker, J.S. Figgis. *J. Am. Chem. Soc.*, **92**, 3794 (1970).
[7] Y.P. Jeannin. *Chem. Rev.*, **98**, 51 (1998).
[8] I. Loose, E. Droste, M. Bössing, H. Pohlmann, M.H. Dickman, C. Rosu, M.T. Pope, B. Krebs. *Inorg. Chem.*, **38**, 2688 (1999).
[9] M. Bössing, A. Noh, I. Loose, B. Krebs. *J. Am. Chem. Soc.*, **120**, 7252 (1998).
[10] D. Rodewald, Y. Jeannin. *C. R. Acad. Sci. Paris Ser. IIc*, 175 (1998).
[11] B. Krebs, E. Droste, M. Piepenbrink, G. Vollmer. *C.R. Acad. Sci. Paris Ser. IIIc*, **3**, 205 (2000).
[12] C. Rosu, M. Rusu, N. Casăn-Pastor, C.J. Gómez-Garciá. *Synth. React. Inorg. Met.-Org. Chem.*, **30**, 369 (2000).
[13] Y. Ozava, Y. Sasaki. *Chem. Lett.*, 923 (1987).
[14] G.L. Xue, H.L. Wang, Z.H. Xie, Q.Z. Shi, J.W. Wang, D.Q. Wang. *Chin. J. Chem.*, **22**, 159 (2004).
[15] D. Rusu, C. Rosu, C. Crăciun, L. David, M. Rusu, Gh. Marcu. *J. Mol. Struct.*, **563–564**, 427 (2001).
[16] D. Rusu, C. Crăciun, A.L. Barra, L. David, M. Rusu, C. Rosu, O. Cozar, G. Marcu. *J. Chem. Soc., Dalton Trans.*, 2879 (2001).
[17] U. Kortz, N.K. Al-Kassem, M.G. Savelieff, N.A. Al-Kadi, M. Sadakane. *Inorg. Chem.*, **40**, 4742 (2001).
[18] F. Robert, M. Leyrie, G. Hervé. *Acta Crystallogr.*, **B38**, 358 (1982).
[19] M. Bössing, I. Loose, H. Pohlmann, B. Krebs. *Chem. Eur. J.*, **3**, 1232 (1997).
[20] T.J.R. Weakley, S.A. Malik. *J. Inorg. Nucl. Chem.*, **29**, 2935 (1967).
[21] X. Zhang, G.B. Jameson, C.J. O'Connor, M.T. Pope. *Polyhedron*, **15**, 917 (1996).
[22] X. Zang, M.Y. Pope, M.R. Chance, G.B. Jameson. *Polyhedron*, **14**, 1381 (1995).
[23] C.M. Tourné, G.F. Tourné, S.A. Malik, T.J.R. Weakley. *J. Inorg. Nucl. Chem.*, **32**, 3875 (1970).